جامعة نايف العربية للعلوم الأمنية
NAIF ARAB UNIVERSITY FOR SECURITY SCIENCES
تأسست ١٩٧٨ Est. 1978

Naif Arab University for Security Sciences
Arab Journal of Forensic Sciences and Forensic Medicine
المجلة العربية لعلوم الأدلة الجنائية والطب الشرعي
https://journals.nauss.edu.sa/index.php/AJFSFM

الجمعية العربية لعلوم الأدلة الجنائية والطب الشرعي
Arab Society for Forensic Sciences and Forensic Medicine

Detection of Etomidate-Class Psychoactive in a Seized Powder: Forensic Confirmation of an Anaesthetic-Derived Substance

الكشف عن مواد نفسانية التأثير من فئة الإيتوميدات في مسحوق مضبوط: التأكيد الجنائي لمادة مشتقة من المخدرات الوريدية

Astha Pandey[1,2*], P. Ajay Soni[2], and Himanshu[2]

[1]Centre of Excellence for Research & Analysis of Narcotic Drugs and Psychotropic Substances, National Forensic Sciences University, Gandhinagar, Gujarat, India

[2]School of Forensic Science, National Forensic Sciences University, Gandhinagar, Gujarat, India

Received 16 Feb. 2026; accepted 5 Apr. 2026; available online 8 Sep. 2026.

Abstract

Illicit drug markets are shifting toward novel sedatives and anaesthetic-derived compounds outside conventional drug classes. Recent reports of etomidate-class substances in seized materials indicate changing patterns of misuse. In this study, a seized powder sample was examined using an orthogonal analytical workflow incorporating chromatographic, mass spectrometric, and spectroscopic techniques. The sample was identified based on retention behaviour, fragmentation patterns, mass accuracy, and complementary structural confirmation from FTIR and ^{1}H NMR data. Etomidate was identified as the major component, with metomidate detected at trace levels. The combined analytical evidence provided strong structural confirmation. These findings highlight the value of orthogonal analytical strategies for the reliable identification of emerging anaesthetic-derived substances in forensic casework.

Keywords: forensic sciences, etomidate, metomidate, emerging psychoactive substances, orthogonal analysis, high-resolution mass spectrometry, forensic drug identification

المستخلص

تشهد أسواق المخدرات غير المشروعة تحولاً نحو المهدئات المستحدثة والمركبات المشتقة من المواد المخدرة (المستخدمة في التخدير الطبي) والتي تقع خارج فئات المخدرات التقليدية. وتشير التقارير الحديثة حول وجود مواد من فئة "الإيتوميدات" (Etomidate-class) في المواد المضبوطة إلى تغير في أنماط إساءة الاستخدام.

في هذه الدراسة، تم فحص عينة من مسحوق مضبوط باستخدام مسار تحليل متعامد (Orthogonal analytical workflow) يدمج بين تقنيات الكروماتوغرافيا، ومطيافية الكتلة، والتقنيات الطيفية. تم تحديد هوية العينة بناءً على سلوك الاحتجاز (Retention behaviour)، وأنماط التجزئة، ودقة الكتلة، بالإضافة إلى التأكيد الهيكلي المتمم باستخدام بيانات مطيافية الأشعة تحت الحمراء (FTIR) والرنين المغناطيسي النووي للبروتون (^{1}H NMR).

أظهرت النتائج أن "الإيتوميدات" هو المكون الرئيسي، مع رصد مادة "الميتوميدات" (Metomidate) بمستويات ضئيلة (أثرية). وقدمت الأدلة التحليلية المجتمعة تأكيداً هيكلياً قوياً. تسلط هذه النتائج الضوء على قيمة استراتيجيات التحليل المتعامد في التحديد الموثوق للمواد المستحدثة المشتقة من المخدرات الطبية في القضايا الجنائية.

الكلمات المفتاحية: علوم الأدلة الجنائية، إيتوميدات، ميتوميدات، المواد النفسانية المستحدثة، التحليل المتعامد، مطيافية الكتلة عالية الدقة، التحديد الجنائي للمخدرات

Production and hosting by NAUSS

* Corresponding Author: Astha Pandey
Email: astha.pandey@nfsu.ac.in

doi: 10.26735/LHHS3642

1. Introduction

In recent years, the scope of illicit drug analysis has expanded beyond conventional narcotic drugs and psychotropic substances [1,2]. Global drug markets are increasingly characterized by the presence of pharmaceutical and other medically used compounds in seized materials [3]. These may appear as substitutes, adulterants, or even as primary psychoactive agents in illicit drugs [2]. As a result, forensic laboratories are increasingly encountering such pharmaceutical and anaesthetic compounds during routine casework [4]. This shift complicates the screening strategies originally developed for conventional drug classes [5].

Etomidate (ethyl 1-(1-phenylethyl)-1H-imidazole-5-carboxylate) is a short-acting, non-barbiturate imidazole-derived hypnotic intravenous anaesthetic [6]. It is widely used for the induction of general anaesthesia due to its rapid onset and minimal cardiovascular depression [7]. The drug produces hypnotic effects mainly through potentiation of γ-aminobutyric acid sub-type A (GABAA) receptors, leading to rapid sedation and loss of consciousness [8]. While its clinical use is well established, recent international reports have documented its detection in non-medical contexts, particularly in East and South-East Asia [9]. Etomidate and its structurally related compounds have been identified in e-liquids, cartridges, tablets, and powder forms [8,10]. In several Asian jurisdictions, including China, Hong Kong, Singapore, Indonesia, Malaysia, Cambodia, and Macao, etomidate-containing vape liquids have been reported in illicit markets under street names such as “space oil,” “ketamine pods,” or “k-pod” [9,11]. These products are intended for inhalation through electronic cigarettes or e-vaporizers and may contain etomidate or related analogues, often in combination with other psychoactive substances such as cannabinoids, ketamine, or designer benzodiazepines [12,13]. Recent reports from the United Nations Office on Drugs and Crime (UNODC) indicate that etomidate and its analogues have been detected in illicit drug samples and toxicology cases globally [3]. Detection of etomidate in tablet and crystalline forms further suggests its emergence beyond liquid formulations in illicit markets [3,10]. This trend indicates emerging misuse of anaesthetic-derived substances in recreational drug markets, potentially involving diversion from legitimate pharmaceutical supply chains or unregulated synthesis of structurally related compounds [3,9].

From a forensic perspective, etomidate is not routinely targeted in standard illicit drug screening [14]. There is limited published literature on the compound, and traditional presumptive tests are unreliable for detecting anaesthetic-derived substances. Many pharmaceutical anaesthetics do not produce characteristic reactions in commonly used presumptive colour tests. As a result, their presence may not be recognized during initial screening [15]. Consequently, reliable identification requires complementary analytical techniques that provide independent molecular and structural information [5].

Forensic drug identification typically follows the guidelines of the Scientific Working Group for the Analysis of Seized Drugs (SWGDRUG) [16]. These guidelines categorize analytical techniques by selectivity: Category A techniques that provide structural information; Category B techniques that offer chemical or physical characteristics; and Category C techniques that provide general or class information. The combined use of techniques from different categories provides independent and complementary analytical evidence, necessary for accurate drug identification [16].

The present case study describes the forensic examination of a seized white powder submitted for

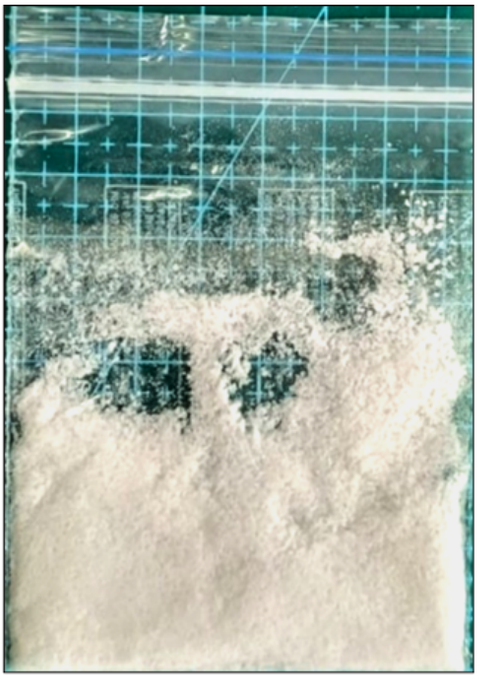

Figure 1- *Seized white powdered sample received for chemical analysis*

chemical analysis. The objective was to determine its composition and achieve confirmatory identification using a structured multi-technique approach. The analytical workflow incorporated both screening and confirmatory techniques, including colour tests, thin-layer chromatography (TLC), direct insertion mass spectrometry (DIMS), gas chromatography–mass spectrometry (GC-MS), high-resolution gas chromatography–high-resolution mass spectrometry (GC-HRMS), Fourier transform infrared spectroscopy (FTIR), and proton nuclear magnetic resonance (^{1}H NMR). The investigation was limited to analytical characterization and did not address the reconstruction of manufacturing pathways or intent.

2. Materials and Methods

2.1. Sample

A seized white coloured powdered sample (Figure 1) was received for forensic chemical analysis. The sample was handled in accordance with standard laboratory procedures for suspected narcotic drugs and psychoactive substances.

2.2. Sample Preparation

50 mg of the sample was accurately weighed and dissolved in 10 mL of methanol (99.9% AR grade, Merck) to obtain a 5 mg/mL solution. The mixture was vortex-mixed until completely dissolved and filtered through a 0.2 μm PVDF syringe filter to remove particulate matter before analysis.

2.3. Preliminary Screening

Colour tests, thin-layer chromatography (TLC), and direct insertion mass spectrometry (DIMS) were used for preliminary screening.

2.3.1. Colour Test

A series of routine presumptive colour tests commonly used in forensic drug analysis were conducted on the sample. The observations from these tests are summarized in Table 1.

2.3.2. Thin-Layer Chromatography (TLC)

Thin-layer chromatography was performed on HPTLC silica gel 60 F_{254} plates. The sample was applied manually as duplicate spots labelled A and B using a glass capillary tube. The plate was developed using ethyl acetate: methanol: ammonia (85:10:5, v/v/v) as the mobile phase. The developed plate was examined under UV light at 254 nm. The observed UV-active spot from one application was excised, and the silica was transferred to a centrifuge tube and extracted with 1 mL of methanol. The suspension was vortex-mixed, sonicated, and centrifuged. The supernatant was subjected to direct insertion mass spectrometry (DIMS). The remaining portion of the plate was subsequently sprayed with acidified iodoplatinate reagent for visualization.

Table 1- *Results of presumptive colour tests performed on the seized sample and their forensic interpretation*

S. No.	Colour Test	Target Class of Drugs	Observation	Interpretation
1	Marquis test	Opiates, amphetamine-type stimulants, and related alkaloidal compounds	No characteristic colour change	No indication of opiates or amphetamine-type substances
2	Mecke's test	Opiates and related opioid compounds	No characteristic colour change	No indication of opiate-type compounds
3	Froehde's test	Opiates and certain synthetic opioids	No characteristic colour change	No indication of opiate-type compounds
4	Scott's test	Cocaine and structurally related tropanes	No characteristic colour change	No indication of cocaine or related tropane compounds
5	Zimmermann's test	Benzodiazepines and ketone-containing drugs	No characteristic colour change	No indication of benzodiazepines or ketone-containing drugs
6	Dille–Koppanyi test	Barbiturates	No characteristic colour change	No indication of barbiturate-type compounds
7	Simon's test	Secondary amines (e.g., MDMA, Meth)	No characteristic colour change	No indication of secondary amine-containing drugs
8	Chen–Kao's test	Ephedrine and pseudoephedrine-type compounds	No characteristic colour change	No indication of ephedrine or pseudoephedrine-type compounds
9	Mandelin test	Wide range of psychoactive substances, stimulants, and common adulterants	No characteristic colour change	No indication of common narcotic and stimulant drugs
10	Ehrlich test	Indole- and tryptamine-containing compounds	No characteristic colour change	No indication of indole- or tryptamine-containing compounds

2.3.3. Direct Insertion Mass Spectrometry (DIMS)

DIMS analysis was performed using a Waters RADIAN ASAP system operated through MassLynx software. Both the methanolic extract of the excised TLC spot (Section 2.3.2) and a diluted sample solution (100 μg/mL) were analyzed. The data were acquired in full-scan mode over an m/z range of 50–1250 in ASAP+ positive ion mode. Nitrogen was used as the desolvation gas at 600 °C, and the cone voltage was varied from 15 to 50 V.

2.4. Confirmatory Analysis

Gas chromatography-mass spectrometry (GC-MS), gas chromatography high-resolution mass spectrometry (GC-HRMS), Fourier-transform infrared (FTIR) spectroscopy, and proton nuclear magnetic resonance (^{1}H NMR) spectroscopy were employed for confirmatory analysis of the sample.

2.4.1. Gas Chromatography–Mass Spectrometry (GC-MS)

GC–MS analysis was performed using a Shimadzu Nexis GC-2030 gas chromatograph coupled with a QP2020 NX mass spectrometer and an AOC-6000 Plus autosampler, operated through LabSolutions software. Chromatographic separation was achieved on an Rtx-5MS low-bleed capillary column (30 m × 0.25 mm I.D. × 0.25 μm film thickness). Helium was used as the carrier gas at a constant flow of 1.5 mL/min. A 1 μL aliquot of

a 25 μg/mL methanolic solution was injected in splitless mode at an injector temperature of 250 °C, with a splitless time of 1 min.

The GC oven temperature program was initiated at 70 °C and held for 2 min, then ramped at 20 °C/min to 200 °C, followed by 7 °C/min to 300 °C, with a 2 min hold, and finally at 25 °C/min to 310 °C, with a 1 min hold. Mass spectrometric detection was accomplished in scan mode over an m/z range of 40–550 with a scan speed of 2000 amu/s, using electron ionization (EI, 70 eV). The ion source and interface temperatures were maintained at 230 °C. A solvent cut time of 2.5 min was applied to prevent detector saturation from the solvent peak.

2.4.2. Gas Chromatography–High-Resolution Mass Spectrometry (GC-HRMS)

GC–HRMS analysis was performed using a Thermo Scientific TRACE 1610 gas chromatograph coupled with an Orbitrap Exploris GC high-resolution mass spectrometer, operated through Chromeleon software. Chromatographic separation was achieved on a TG-5SilMS capillary column (30 m × 0.25 mm I.D. × 0.25 μm film thickness). Helium was used as the carrier gas at a constant flow rate of 1.0 mL/min. A 2 μL aliquot of a 10 μg/mL methanolic solution was injected in splitless mode with a splitless time of 1 min and an injector temperature of 280 °C.

The GC oven temperature program was initiated at 70 °C and held for 2 min, then ramped at 20 °C/min to 200 °C, followed by 7 °C/min to 300 °C, with a 2 min hold, and finally at 25 °C/min to 310 °C, with a final 2 min hold. Mass spectrometric detection was achieved using electron ionization (EI, 70 eV) in high-resolution full-scan mode (m/z 50–550) at a resolving power of 60,000 (FWHM at m/z 200) for accurate mass determination.

2.4.3. Fourier-Transform Infrared (FTIR)

FTIR analysis was performed using a Bruker INVENIO X spectrometer equipped with a diamond ATR accessory, operated through OPUS software. A small amount of the sample was directly placed on the ATR crystal and gently pressed to ensure good contact with the ATR crystal. Spectra were recorded over 4000–400 cm-1 at 4 cm-1 resolution using 64 scans in transmittance mode.

2.4.4. Proton Nuclear Magnetic Resonance Spectroscopy (^{1}H NMR)

^{1}H NMR spectra were recorded on a Magritek Spinsolve 80 MHz benchtop NMR spectrometer using deuterated chloroform (CDCl3, 99.8% atom D stabilized, SRL) as solvent. A fresh portion of the sample (approximately 30 mg) was dissolved in 0.6 mL of CDCl3 to ensure adequate signal intensity at low field (80 MHz). The solution was transferred to a 5 mm NMR tube for analysis. Spectra were acquired with 128 scans, 90° pulse angle, acquisition time of 3.2 s, and repetition time of 30 s. Spectral processing and interpretation were performed using MestReNova (Mnova, Mestrelab Research) software.

3. Results and Discussion

3.1. Preliminary Analytical Findings

Preliminary screening of the seized sample using routine colour tests, summarized in Table 1, did not show characteristic reactions linked to commonly encountered narcotic drugs or psychotropic substances. These observations were interpreted in accordance with established forensic protocols described in standard reference manuals and guidelines [17–20]. The absence of a characteristic colour response does not exclude the presence of a drug; however, it indicates that the sample does not correspond to drug classes typically identified using

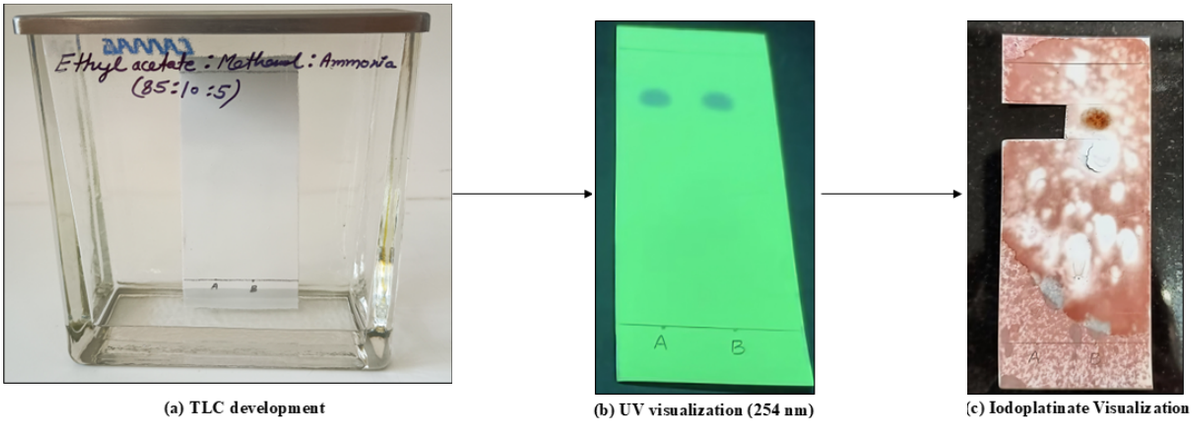

Figure 2- *TLC analysis of the seized sample showing a single UV-active spot at 254 nm and corresponding brown spot after visualization with acidified iodoplatinate reagent*

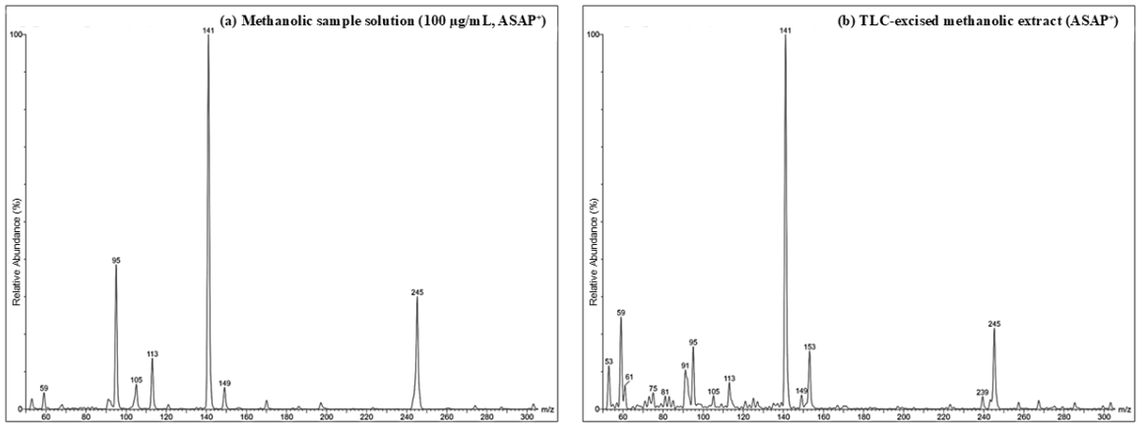

Figure 3- *DIMS ASAP $^{+}$ mass spectra of (a) methanolic sample solution (100 µg/mL) and (b) TLC-excised methanolic extract, both showing a prominent ion at m/z 245 ($[M+H]^{+}$)*

routine presumptive colour tests [15], necessitating further confirmatory analysis.

Thin-layer chromatography (TLC) analysis under UV light at 254 nm showed a single, well-defined quenching spot in both duplicate applications A and B (Figure 2). The spots were horizontally aligned, indicating identical migration, with a retention factor (Rf) of 0.8 in the ethyl acetate: methanol: ammonia (85:10:5, v/v/v) mobile phase. After spraying with acidified iodoplatinate reagent, the plate developed a brown spot at the same Rf. No additional major spots were apparent under UV or after chemical visualization. The TLC observations are summarized in Table 2. One of the duplicate applications was excised for DIMS analysis, while the other was subjected to chemical visualization. The consistent migration pattern and the presence of a single major spot under both visualization conditions

suggest that a single major component predominated under the applied TLC conditions.

The ASAP+ mass spectrum obtained from direct insertion mass spectrometry showed a high-intensity ion at m/z 245 (Figure 3a and 3b), indicative of a protonated molecular ion $[M+H]^{+}$ corresponding to a compound of nominal mass 244 Da. This finding is consistent with reported precursor ion data for etomidate (m/z 245.1) obtained under soft ionization conditions [17]. Comparable spectra were obtained

from both the methanolic extract of the excised TLC spot and the diluted sample solution, confirming the presence of the same major component in both preparations. Additional fragment ions were observed at m/z 141, 95, 105, and 113, consistent with reported fragmentation behaviour of etomidate and related imidazole-derived compounds [10]. The full-scan spectrum did not reveal additional major molecular ions, indicating that a single predominant component was present under the applied acquisition conditions. These observations indicate the presence of a compound with a nominal mass of 244 Da and guided the subsequent confirmatory analysis.

3.2. Chromatographic Mass Confirmation

Chromatographic analysis of the seized sample by GC-MS showed two well-resolved peaks (Figure 4). The peak at 11.16 min was predominant and assigned to etomidate, while the earlier eluting peak at 10.61 min corresponded to metomidate and was present at lower abundance, in agreement with the component distribution observed in the GC-HRMS chromatogram (Figure 7).

The electron ionization mass spectrum corresponding to the predominant peak at 11.16 min (Figure 5a) indicates a compound with a nominal mass of 244 Da. The spectrum was dominated by the fragment ion at m/z 105, accompanied by ions at m/z 77 and 95. These fragments are characteristic of phenyl-containing substructures and are consistent

Table 2- *TLC observations of the seized sample under UV light and after chemical visualization*

S. No.	Sample/Application	Visualization Method	Observation	Rf Value
1	Spot A	UV at 254 nm	Single compact UV-quenching spot observed	0.8
2	Spot B	UV at 254 nm	Single compact UV-quenching spot observed	0.8
3	Spot B (plate after excision)	Acidified Iodoplatinate Reagent Spray	Brown spot observed at the same position	0.8

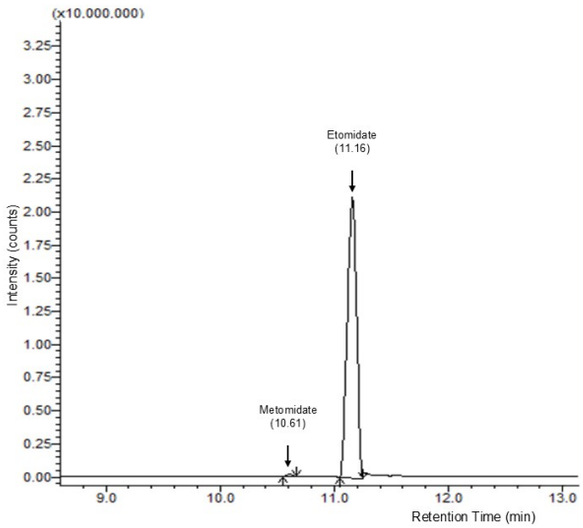

Figure 4- *GC–MS chromatogram of the seized sample showing two resolved peaks corresponding to etomidate (11.16 min) and metomidate (10.61 min)*

with reported EI fragmentation behaviour of phenyl-substituted imidazole anaesthetics [10,18]. The fragment at m/z 105 corresponds to the benzylic-type cation formed through cleavage adjacent to the phenyl substituent, while m/z 77 represents the phenyl cation produced by further rearrangement of the aromatic system. The ion at m/z 95 likely arises from secondary fragmentation of the aromatic system. An additional fragment at m/z 198-199 was also observed, consistent with cleavage involving the ester-containing moiety of the molecule. This is in close agreement with reported fragment ions for etomidate, where analogous fragments are observed around m/z 199, with minor variations attributable to fragmentation pathways and hydrogen rearrangement processes [18]. The proposed

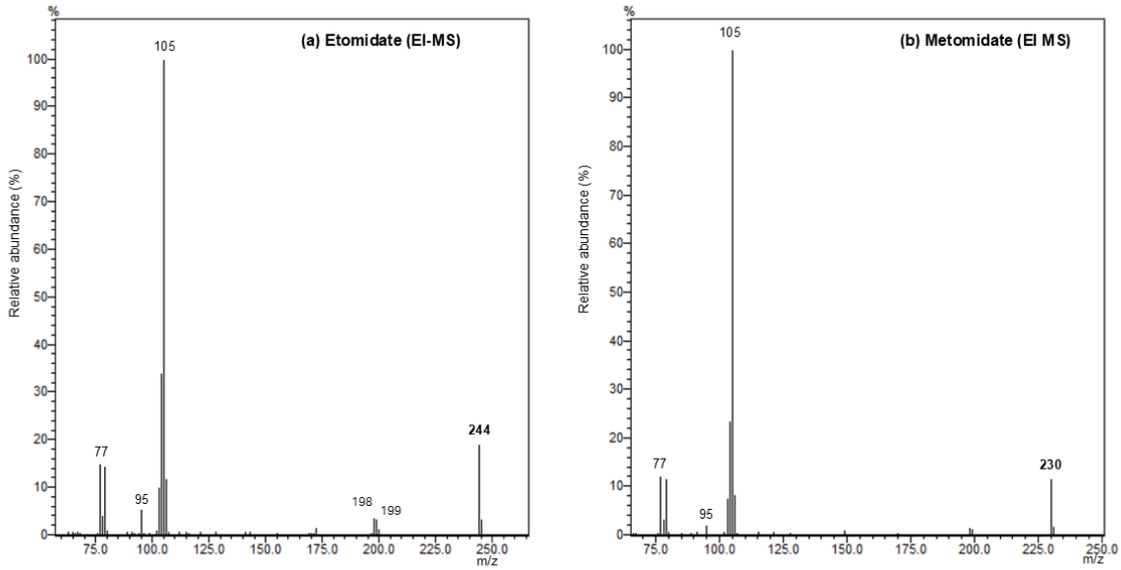

Figure 5- *EI mass spectra obtained from GC–MS analysis of (a) etomidate and (b) metomidate, showing characteristic fragment ions*

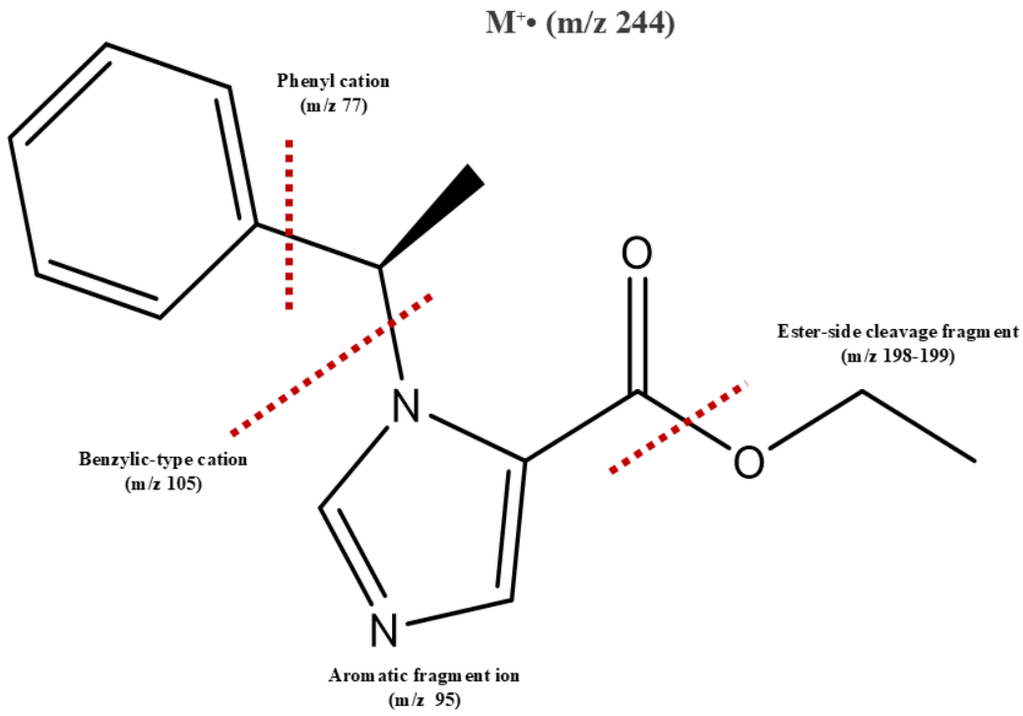

Figure 6- *Proposed EI MS fragmentation of etomidate illustrating the formation of diagnostic fragment ions at m/z 244, 105, 95, 77, and 198-199*

fragmentation scheme illustrating the formation of the diagnostic m/z 105, 95, 77, and 198-199 ions is presented in Figure 6. Comparison with library data also showed a high similarity to etomidate, supporting its identification as the major component.

The earlier eluting peak at 10.61 min (Figure

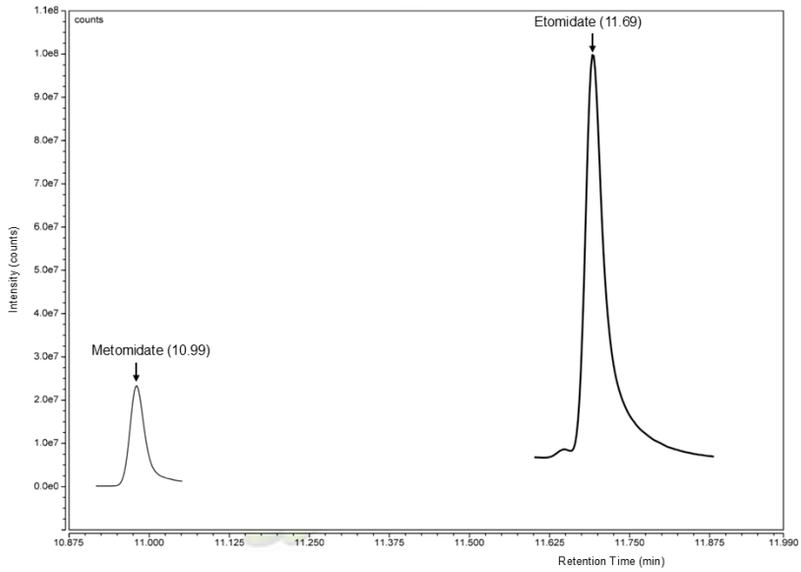

Figure 7- *GC–HRMS extracted ion chromatogram (XIC) showing two peaks corresponding to metomidate (10.99 min) and etomidate (11.69 min)*

Table 3- *Accurate mass measurements and diagnostic fragment ions obtained from GC–HRMS analysis of etomidate and metomidate*

Compound	Molecular formula	RT (min)	Molecular ion from extracted-ion confirmation (m/z)	Diagnostic fragment ions from apex spectrum (m/z)
Etomidate	$C_{14}H_{16}N_{2}O_{2}$	11.69	244.1212	105.06972, 104.06209, 77.03858, 198.07884
Metomidate	$C_{13}H_{14}N_{2}O_{2}$	10.99	230.1055	105.06976, 104.06211, 77.03820

5b) showed a mass spectrum consistent with a compound of nominal mass 230 Da, with similar diagnostic fragments at m/z 105 and 77. The 14 Da mass difference between the two components indicates that they are structurally related analogues. Such a difference is consistent with the presence or absence of a single methylene ($–CH_2–$) unit, suggesting a shared core structure. Library comparison revealed that this minor component was metomidate, present at trace levels compared to the main compound [8]. No other major chromatographic peaks of similar intensity were observed under the applied GC–MS conditions, and the minor earlier eluting peak was interpreted as a structurally related coexisting analogue rather than a separate impurity.

To further support these identifications, gas chromatography–high resolution mass spectrometry (GC-HRMS) analysis was performed. Two chromatographic peaks were again observed at approximately 10.99 min and 11.69 min (Figure 7), corresponding to metomidate and etomidate, respectively. Accurate mass measurements showed ions at m/z 230.1055 and 244.1212 for the earlier and later peaks, consistent with the expected molecular ions of metomidate and etomidate, with mass errors within ±5 ppm. These values were derived from high-resolution extracted ion chromatogram (XIC) data and confirmed through the corresponding ion table generated during HRMS data processing (Table 3). This level of mass accuracy supports reliable elemental composition assignment and reduces the likelihood of isobaric interferences.

In addition to the molecular ions, both spectra

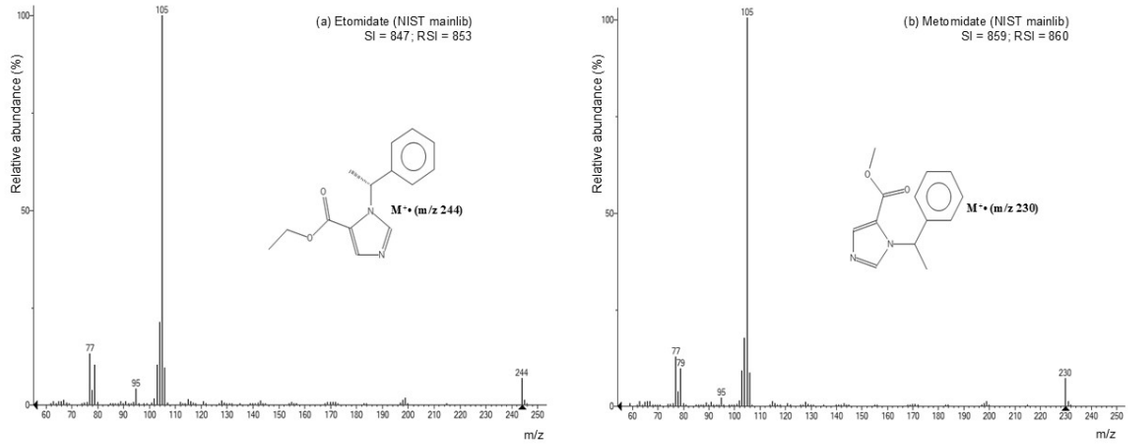

Figure 8- *EI mass spectra of (a) etomidate and (b) metomidate obtained from GC–HRMS data and compared with reference spectra*

showed common high-resolution fragment ions at approximately m/z 105.06972, 104.06209, and 77.03858, arising from the phenyl-substituted imidazole framework [10]. The consistency of these fragment ions across both components further supports their structural similarity. The relative ion-abundance relationships among the selected confirming ions were also consistent with accepted forensic mass-spectrometric identification criteria [16]. Furthermore, the agreement between experimental and theoretical exact masses within low ppm error provided additional confidence in elemental composition assignment and compound identity [19]. The observed fragmentation pattern and molecular ion information were consistent with the corresponding reference EI spectra (Figure 8a and 8b), with high similarity scores obtained for metomidate (SI 859; RSI 860) and etomidate (SI 847; RSI 853), further confirming the assigned identities [16].

Collectively, GC-MS and GC-HRMS findings demonstrated chromatographic separation of two structurally related compounds with a nominal mass difference of 14 Da, consistent fragmentation behaviour, accurate-mass confirmation, and strong library agreement. These findings support the conclusion that etomidate is the predominant component of the seized sample, with metomidate as a minor coexisting compound.

3.3. Spectroscopic Structural Confirmation

Structural confirmation was further supported by Fourier-transform infrared (FTIR) spectroscopy and proton nuclear magnetic resonance (^{1}H NMR), which provided complementary vibrational and proton environment information.

The ATR–FTIR spectrum (Figure 9) showed a strong absorption band at 1707 cm-1, characteristic of ester C=O stretching, indicating conjugation with an imidazole containing system [24,25]. The aromatic C–H stretching bands observed at 3132 and 3099 cm-1, together with the aliphatic C–H stretching band at 2974 cm-1, confirmed the presence of both aromatic and aliphatic moieties within the molecule [26]. Bands at 1524 and 1497 cm-1 correspond to aromatic ring skeletal vibrations, with contributions from C=C and C=N stretching associated with the imidazole moiety [25,26]. Characteristic ester C–O stretching bands were present at 1212 and 1169 cm-1 [24]. Additional bands at 1455 and 1371 cm-1 correspond to aliphatic C–H deformation modes of methyl and methylene groups [26]. In the fingerprint

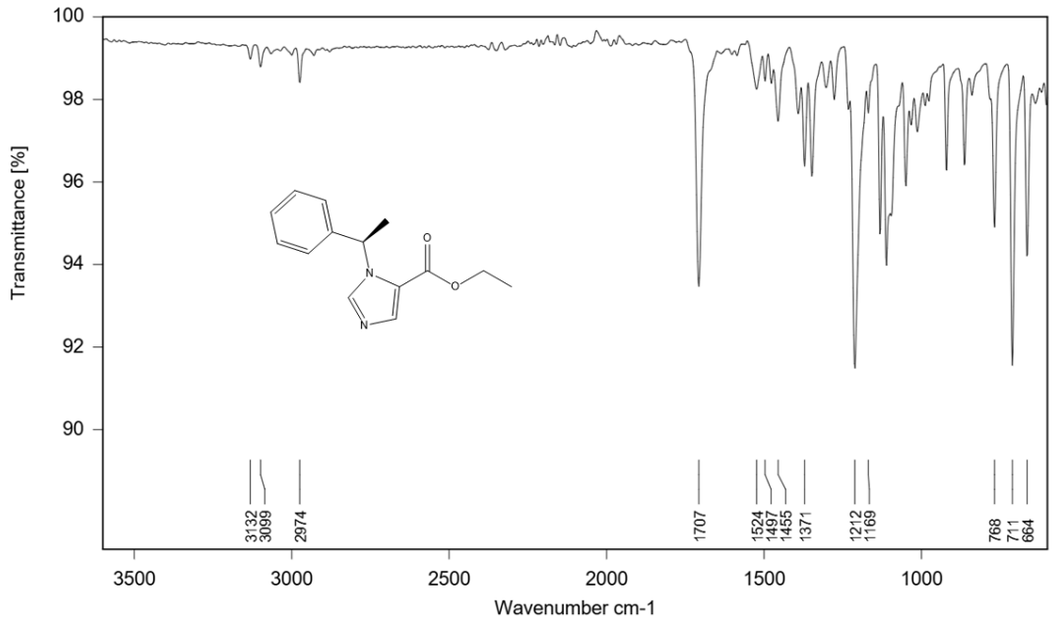

Figure 9- *ATR–FTIR spectrum of the sample showing characteristic bands corresponding to ester, aromatic, and imidazole functional groups*

region, absorptions at 768, 711, and 664 cm-1 are attributed to out-of-plane C–H bending vibrations of a substituted phenyl ring, further supporting the presence of a monosubstituted aromatic system [21].

The overall infrared profile aligns with the expected functional groups of etomidate ($C_{14}H_{16}N_2O_2$) and supports the identification established through chromatographic and mass spectrometric analysis.

The ^{1}H NMR spectrum (80 MHz, $CDCl_3$) of the sample (Figure 10) showed resonances consistent with the expected proton environments of etomidate. A downfield resonance at δ ~7.8-7.9 ppm (2H) was assigned to the imidazole proton [24], while a complex multiplet region δ ~7.2-7.5 ppm (5H) corresponded predominantly to the aromatic protons of the phenyl ring. The ethyl ester functionality was identified by its characteristic splitting pattern, consisting of a methylene quartet (–OCH_2–) at δ ~4.22-4.49 ppm (2H) and terminal methyl triplet at δ ~1.32-1.49 ppm (3H), consistent with reported ^{1}H NMR characteristics of etomidate and structurally related compounds [24,25]. A doublet at δ ~1.9-2.3 ppm (3H) was assigned to the methyl group coupled to the adjacent methine proton of the 1-phenylethyl moiety [24]. A weak, partially resolved signal was observed at δ ~6.3-6.6 ppm (1H), tentatively corresponding to the chiral methine proton, which could not be clearly resolved due to the limited spectral resolution of the low-field benchtop instrument.

The relative integration values obtained directly from the spectrum were approximately 1.98, 5.08, 0.99, 1.99, 2.95, and 3.03, corresponding to a total of 16 protons. These values are in close agreement with the expected proton distribution of etomidate ($C_{14}H_{16}N_2O_2$), giving an approximate ratio of 2:5:1:2:3:3 across the observed proton environments [23,26]. Minor deviations from ideal integer values are attributed to signal overlap and the limited resolution of the 80 MHz benchtop system.

The observed splitting patterns, including the

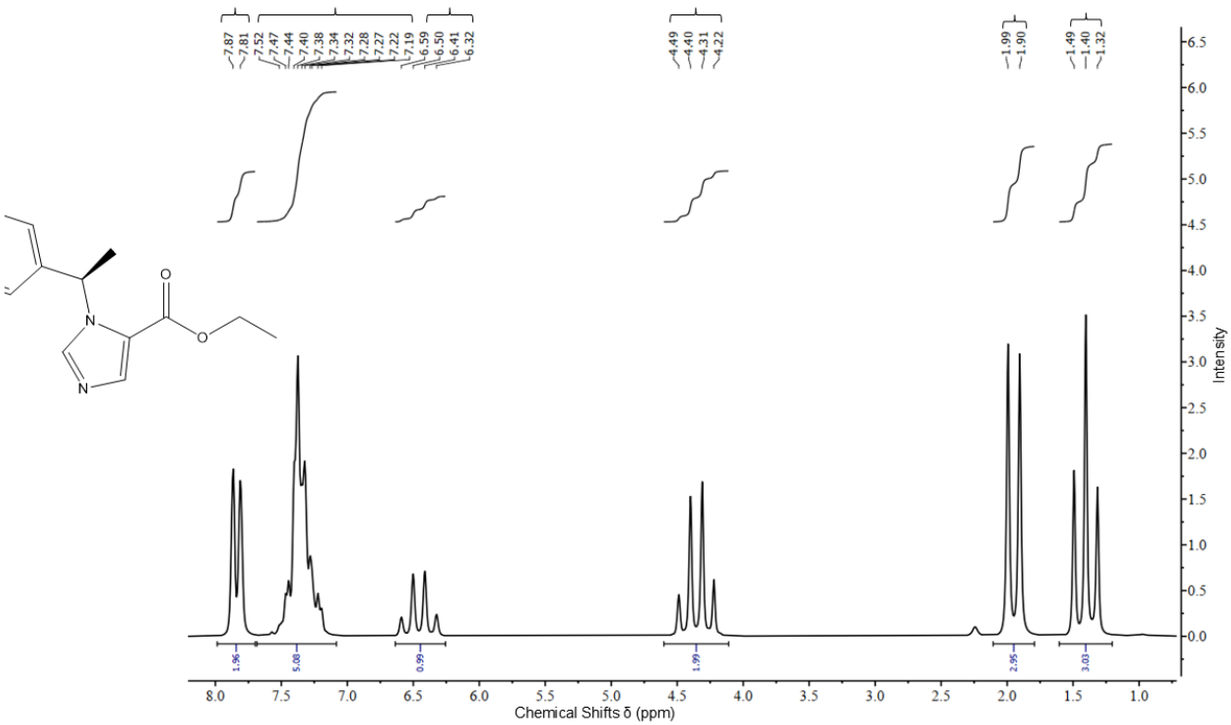

Figure 10- *¹H NMR spectrum of the sample showing proton environments consistent with etomidate.*

quartet–triplet for the ethyl group and the doublet of the chiral methyl group, were consistent with the expected coupling relationships [28,10]. Overall, the chemical shift positions and integration values are in good agreement with reported ¹H NMR data for etomidate and related imidazole anaesthetics [24], further supporting structural consistency with the chromatographic and mass spectrometric findings.

The analytical results satisfy the identification criteria recommended by the Scientific Working Group for the Analysis of Seized Drugs (SWGDRUG). The workflow integrates screening, separation, and structural techniques consistent with SWGDRUG principles of orthogonal forensic identification, including presumptive testing, chromatographic separation, mass spectrometry, FTIR, and ¹H NMR [16].

4. Conclusion

The seized sample was examined using chromatographic, mass spectrometric, and spectroscopic techniques. Preliminary colour tests did not show characteristic reactions for commonly encountered drug classes, indicating the need for further confirmatory analysis, while thin-layer chromatography revealed a single major component under the applied conditions. Direct insertion mass spectrometry (DIMS) indicated a compound with a nominal mass of 244 Da, guiding subsequent analysis. GC–MS showed two distinct peaks, and the corresponding EI mass spectra exhibited characteristic fragmentation patterns. Accurate mass measurements from GC–HRMS, together with library matching, supported the identification of etomidate as the major component and its structural analogue metomidate in trace amounts. Further confirmation was obtained through FTIR and ¹H NMR, which were consistent with the expected functional groups and proton environments of etomidate. Collectively, the integrated analytical findings provide strong and

consistent evidence for the presence of etomidate as the major component, along with trace levels of metomidate in the seized material.

This study highlights the importance of recognising anaesthetic-derived compounds in routine seized drug casework, where they may not be readily detected by conventional screening methods. The findings also indicate a shift in the chemical profile of illicit drug markets toward pharmaceutical-derived substances beyond traditional drug classes, underscoring their growing relevance for forensic and regulatory monitoring. Accordingly, these observations emphasize the need for comprehensive, multi-technique analytical strategies in forensic laboratories to ensure such compounds are not overlooked during routine analysis.

5. LIMITATIONS

This study was limited to the qualitative identification and structural confirmation of the seized sample. Quantitative estimation, detailed impurity profiling, reconstruction of manufacturing pathways, and source attribution were not undertaken in the present study and may be explored in future work.

Author Contributions

Astha Pandey: Conceptualization, supervision, and critical review of the manuscript. P. Ajay Soni: Data interpretation support and manuscript review. Himanshu: Experimental work, data acquisition, analysis, visualization, and manuscript drafting.

Acknowledgments

The authors acknowledge the Centre of Excellence for Research & Analysis of Narcotic Drugs and Psychotropic Substances, National Forensic Sciences University, Gandhinagar Campus, Gujarat, India, for providing the necessary laboratory and instrumental facilities.

Source of Funding

The authors received no financial support for the research, authorship or publication of this article.

Conflict of Interest

The authors declare no conflicts of Interest.

References

1. Dimić D. Emerging Novel Psychoactive Substances (2020–2025): GC-MS Approaches for Separation, Detection, and Characterization. Chemosensors. 2025 Dec 9;13(12):426–426. doi:10.3390/chemosensors13120426
2. Meyer M, Westenberg JN, Jang KL, Choi F, Schreiter S, Mathew N, et al. Shifting drug markets in North America - a global crisis in the making? International Journal of Mental Health Systems. BioMed Central; 2023. doi:10.1186/s13033-023-00601-x
3. UNODC: Synthetic Drugs in East_and Southeast Asia 2025. Regional Office for Southeast Asia and the Pacific.
4. Qian Z, Liu C, Huang J, Deng Q, Hua Z. Identification of the designer benzodiazepine 8-chloro-6-(2-fluorophenyl)-1-methyl-4H-[1,2,4]triazolo[4,3-a][1,4]benzodiazepine (flualprazolam) in an anesthesia robbery case. Forensic Toxicology. 2019 Sep 30;38(1):269–76. doi:10.1007/s11419-019-00501-1
5. Brown K, Dennany L. Novel Detection Approaches to Tackle the Challenges of Complex Matrices for Alternative Drugs and New Psychoactive Substances. In: The Royal Society of Chemistry eBooks. Royal Society of Chemistry; 2021. p. 41–71. doi:10.1039/9781839160912-00041
6. Raines DE. Etomidate and Etomidate Analogues: Molecular Pharmacology and Behavioral Actions. In: Absalom AR, Mason KP, editors. Total Intravenous Anesthesia and Target Controlled Infusions: A Comprehensive Global Anthology. Cham:

Springer International Publishing; 2017. p. 209–19. doi:10.1007/978-3-319-47609-4_12

7. Valk BI, Struys MMRF. Etomidate and its Analogs: A Review of Pharmacokinetics and Pharmacodynamics. Clin Pharmacokinet. 2021 Oct 1;60(10):1253–69. doi:10.1007/s40262-021-01038-6
8. Zhang X, Li Y, Liu J, Pan Z, Chen Y, Wang M, et al. Identification of two novel imidazole-derived GABA agonists butomidate and tf-etomidate in e-cigarette liquids. Forensic Toxicol. 2026 Jan 1;44(1):47–60. doi:10.1007/s11419-025-00732-5
9. Gao T, Jin M, Alibudbud R, Assanangkornchai S, Sun Y, Lu L. Etomidate misuse: a digital era threat to youth and a call for anticipatory control. 2025. doi:10.1016/s2215-0366(25)00267-6
10. Fan Y, Chen X, Wu H, Ke X, Chen H, Xu Y, et al. Leveraging mass spectrometry fragmentation patterns for accelerated screening and structural elucidation of new etomidate analogues in suspect samples. Journal of Pharmaceutical and Biomedical Analysis. 2025 Jun 16;265:117023–117023. doi:10.1016/j.jpba.2025.117023
11. Increasing detections of etomidate and analogues on illicit drug markets is becoming a global concern [Internet]. 2025. Available from: https://www.unodc.org/LSS/Announcement/Details/8774c132-4b30-477c-9ceb-46ce384223fd
12. Wu W, Xia C, Gan L, Liao S, Yan Y. Etomidate-induced hypokalemia in electronic cigarette users: two case reports and literature review. Front Endocrinol. 2024 May 30;15. doi:10.3389/fendo.2024.1321610
13. Lin CH, Lin CH. From benzodiazepine to etomidate: A risky novel psychoactive substance. Indian Journal of Psychiatry. 2024 Oct;66(10):981. doi:10.4103/indianjpsychiatry.indianjpsychiatry_735_24
14. Bruni AT, Rodrigues CHP, Santos C dos, Castro JS, Mariotto LS, Sinhorini L. Analytical Challenges for Identification of New Psychoactive Substances: A Literature-Based Study for Seized Drugs. Brazilian Journal of Analytical Chemistry. 2021 Sep 29. doi:10.30744/brjac.2179-3425.rv-41-2021
15. Philp M, Fu S. A review of chemical 'spot' tests: A presumptive illicit drug identification technique. Drug Testing and Analysis. 2017 Sep 15;10(1):95–108. doi:10.1002/dta.2300
16. SWGDRUG: Recommendations of the Scientific Working Group for the Analysis of Seized Drugs (SWGDRUG). Version 8.2; 2024 [Internet]. Available from: https://www.swgdrug.org/
17. Laboratory and Scientific Section. Rapid Testing Methods of Drugs of Abuse. Vienna: United Nations Office on Drugs and Crime; 1994.
18. Color Test Reagents/Kits for Preliminary Identification of Drugs of Abuse, NIJ Standard-0604.01, National Institute of Justice. U.S. Department of Justice, Office of Justice Programs, National Institute of Justic; 2000.
19. Controlled Substances Procedures Manual. Virginia: Department of Forensic Science, Virginia; 2025.
20. Narcotics Manual. New Delhi: Directorate of Forensic Science, Ministry of Home Affairs, Govt. of India; 2024.
21. Smith BC. Infrared Spectral Interpretation: A Systematic Approach. Boca Raton: CRC Press; 2018. 288 p. doi:10.1201/9780203750841
22. Coates J. Interpretation of Infrared Spectra, A Practical Approach. In: Wiley Online Library Encyclopedia of Analytical Chemistry: Applications, Theory and Instrumentation. 2006. doi:10.1002/9780470027318.a5606
23. Pavia DL, Lampman GM, Kriz GS, Vyvyan JR. Introduction to Spectroscopy. Cengage Learning; 2013.
24. Pejo E, Santer P, Jeffrey S, Gallin H, Husain SS, Raines DE. Analogues of Etomidate: Modifications Around Etomidate's Chiral Carbon and the Impact on In Vitro and In Vivo Pharmacology. Anesthesiology. 2014 Aug;121(2):290–301. doi:10.1097/ALN.0000000000000268 PubMed Central PMCID: PMC4121658.

25. Fulmer GR, Miller AJM, Sherden NH, Gottlieb HE, Nudelman A, Stoltz BM, et al. NMR Chemical Shifts of Trace Impurities: Common Laboratory Solvents, Organics, and Gases in Deuterated Solvents Relevant to the Organometallic Chemist. Organometallics. 2010 May 10;29(9):2176–9. doi:10.1021/om100106e

26. Elyashberg M. Identification and structure elucidation by NMR spectroscopy. TrAC Trends in Analytical Chemistry. 2015;69:88–97. doi:10.1016/j.trac.2015.02.014.